

Electronic phase transitions in $\text{Pr}_{0.5}\text{Ca}_{0.5}\text{MnO}_3$ epitaxial thin films revealed by resonant soft x-ray scattering

H. Wadati,^{1,2,*} J. Geck,³ E. Schierle,⁴ R. Sutarto,¹ F. He,⁵ D. G. Hawthorn,⁶
M. Nakamura,⁷ M. Kawasaki,^{2,7} Y. Tokura,^{2,7} and G. A. Sawatzky¹

¹*Department of Physics and Astronomy, University of British Columbia, Vancouver, British Columbia V6T 1Z1, Canada*

²*Department of Applied Physics and Quantum-Phase Electronics Center (QPEC),
University of Tokyo, Hongo, Tokyo 113-8656, Japan*

³*IFW Dresden, P.O. Box 270116, D-01171 Dresden, Germany*

⁴*Helmholtz-Zentrum Berlin für Materialien und Energie Albert-Einstein-Straße 15, 12489 Berlin, Germany*

⁵*Canadian Light Source, University of Saskatchewan, Saskatoon, Saskatchewan S7N 0X4, Canada*

⁶*Department of Physics and Astronomy, University of Waterloo, Waterloo, Ontario N2L 3G1, Canada*

⁷*Cross-Correlated Materials Research Group (CMRG), ASI, RIKEN, Wako 351-0198, Japan*

(Dated: November 22, 2011)

We report the study of magnetic and orbital order in $\text{Pr}_{0.5}\text{Ca}_{0.5}\text{MnO}_3$ epitaxial thin films grown on $(\text{LaAlO}_3)_{0.3}\text{-(SrAl}_{0.5}\text{Ta}_{0.5}\text{O}_3)_{0.7}$ (LSAT) (011)_c. In a new experimental approach, the polarization and energy dependence of resonant soft x-ray scattering are used to reveal significant modifications of the magnetic order in the film as compared to the bulk, namely (i) a different magnetic ordering wave vector, (ii) a different magnetic easy axis and (iii) an additional magnetic reordering transition at low temperatures. These observations indicate a strong impact of the epitaxial strain on the spin order, which is mediated by the orbital degrees of freedom and which provides a promising route to tune the magnetic properties of manganite films. Our results further demonstrate that resonant soft x-ray scattering is a very suitable technique to study the magnetism in thin films, to which neutron scattering cannot easily be applied due to the small sample volume.

Hole-doped perovskite manganites $R_{1-x}A_x\text{MnO}_3$, where R is a rare-earth ($R = \text{La}, \text{Nd}, \text{Pr}$) and A is an alkaline-earth atom ($A = \text{Sr}, \text{Ba}, \text{Ca}$) have attracted much attention because they exhibit remarkable physical properties such as colossal magnetoresistance and complex electronic ordering phenomena [1–8]. For the latter, the half-doped manganites provide a particular prominent and extensively studied example, namely the so-called CE-phase [9]. This phase is commonly discussed in terms of cooperative spin, charge and orbital order, where ferromagnetic zig-zag chains are formed, which are coupled antiferromagnetically to each other. Notwithstanding intensive research, however, the detailed microscopic structure of the electronic order remains to be fully understood. In particular, the question whether charge ordering really exists and, in case it does, whether it is centered on oxygen or manganese is currently discussed vigorously in the literature [10, 11].

Potential applications of manganites heavily rely on their physical properties in the form of thin films grown on a substrate. Epitaxial thin films are usually strained to some degree and the interfaces may introduce modifications of the properties. It is therefore very important to investigate and understand the electronic modifications in doped manganite films, which can be dramatic. For example, it was recently shown that epitaxial strain effects can control charge ordering (CO) in thin films of Mn-oxides [12, 13]. A transition between CO and ferromagnetic metallic states was observed in $\text{Nd}_{0.5}\text{Sr}_{0.5}\text{MnO}_3$ films on SrTiO_3 (011)_c substrates, whereas $\text{Nd}_{0.5}\text{Sr}_{0.5}\text{MnO}_3$ films on SrTiO_3 (001)_c sub-

strates exhibit only insulating behavior at all temperatures [12]. Here the substrate orientation is given in the standard cubic notation. Also in $\text{Pr}_{0.5}\text{Ca}_{0.5}\text{MnO}_3$ thin films, epitaxial strain strongly affects the electronic properties. Previous studies have shown that $\text{Pr}_{0.5}\text{Ca}_{0.5}\text{MnO}_3$ films grown epitaxially on $(\text{LaAlO}_3)_{0.3}\text{-(SrAl}_{0.5}\text{Ta}_{0.5}\text{O}_3)_{0.7}$ (LSAT) (011)_c substrate exhibit a CO transition around 220 K, similar to bulk samples, while $\text{Pr}_{0.5}\text{Ca}_{0.5}\text{MnO}_3$ films on LSAT (001)_c substrates has a much higher CO transition temperature around 300K [13].

Here we present a resonant soft x-ray scattering (RSXS) study of the electronic order in $\text{Pr}_{0.5}\text{Ca}_{0.5}\text{MnO}_3$ thin films grown epitaxially on LSAT (011), which implies that the microscopic magnetic order in films can differ significantly from that of the corresponding bulk materials. Our results indicate that epitaxial strain couples to the spin order via the orbital degrees of freedom, which provides a unique way to tune the magnetic properties of doped manganite films.

$\text{Pr}_{0.5}\text{Ca}_{0.5}\text{MnO}_3$ thin films were grown on LSAT (011)_c substrates by pulsed laser deposition. Details of the fabrication and characterization of the thin films were described elsewhere [13]. RSXS experiments at the Mn 2p edge were performed at the BESSY undulator beamline UE 46-PGM and 10ID-2 (REIXS) of the Canadian Light Source [14]. Scattering spectra were measured using horizontally (π) or vertically polarized (σ) light. We will refer to the resonant intensity measured in the $\pi \rightarrow \sigma'$, π' and $\sigma \rightarrow \sigma'$, π' channels as I_π and I_σ , respectively. The pressure during measurements were below 5×10^{-9} Torr, and

the temperature was varied between room temperature (RT) and 25 K. We also performed x-ray absorption spectroscopy (XAS) measurements in the total-electron-yield (TEY) mode.

In the following, the (HKL) -indexes for the film reflections and directions refer to the orthorhombic unit cell of the PCMO-film [13]. At this point it is important to realize that the PCMO-films contain structural domains with interchanged a - and b -axes – so-called twin domains. We will refer to these twin domains as $D1$ and $D2$, respectively, and designate the reflections and directions of these domains with a corresponding index. Using this convention, the orthorhombic $(100)_{D1}$ and $(011)_{D1}$ directions were parallel to the scattering plane as shown in Fig. 1 (a), which corresponds to $(010)_{D2}$ and $(101)_{D2}$ of the other twin domain. In a scattering experiment, the diffraction patterns of $D1$ and $D2$ are superimposed. This means that close to the position of $(H, 0, 0)_{D1}$, the $(0, H, 0)_{D2}$ reflection can be observed, if it occurs as well. However, because $a \neq b$, these two reflections possess slightly different scattering angles. This orthorhombic peak splitting enables to identify the $(H, 0, 0)_{D1}$ and $(0, H, 0)_{D2}$ reflections from the different domains.

Figure 1 (c) shows the temperature dependence of the resonant intensity measured around the $(1/2, 0, 0)_{D1}$ position with incoming π -polarization. The photon energy was set to 643.6 eV, which corresponds to the Mn $2p$ absorption peak. A clear peak appears around 210 K and strongly gains intensity with decreasing temperature. This result is in good agreement with the charge/orbital-ordering transition temperature $T_{CO/OO} = 220$ K reported in Ref. [13]. The peak widths show almost no change with temperature, demonstrating that the ordering is always long-ranged below $T_{CO/OO}$ and that the domain sizes do not exhibit a significant temperature dependence.

The position of the superlattice peak as a function of temperature is shown in Fig. 1 (d). A clear shift of the peak position is observed at the magnetic ordering temperature $T_N = 150$ K, even though the lattice parameters do not change significantly at this temperature [13]. Above T_N and below $T_{CO/OO}$, the peak position corresponds exactly to the $(1/2, 0, 0)_{D1}$ reflection, identifying it as the superlattice reflection due to the orbital order in $D1$. Note that the orbital order causes a doubling of the orthorhombic a -axis only, i.e., the $(0, 1/2, 0)_{D2}$ does not occur in the orbital ordered phase. However, with the onset of magnetic order below T_N , the peak position jumps to $(0, 1/2, 0)_{D2}$, implying that the observed intensity is now due to the magnetic order in twin domain $D2$. As we will discuss further below, the orbital scattering of $D1$ still exists below T_N , but its intensity is much smaller than the magnetic scattering of $D2$.

Figure 2 shows the photon-energy dependence of the intensity observed at the $(1/2, 0, 0)_{D1}$ position across the Mn $2p$ edges at various temperatures using π and σ po-

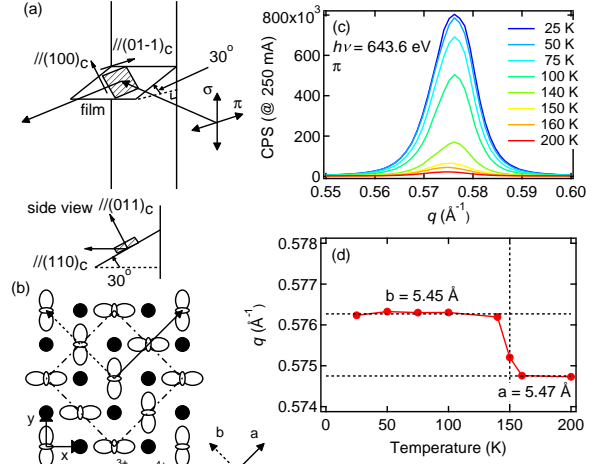


FIG. 1: (Color online) Temperature dependence observed at the $(1/2, 0, 0)_{D1}$ position (c). The experimental geometry is shown in panel (a). Panel (b) shows the schematic drawing of the charge-orbital ordering. The arrow marks the directions for the orbital ordering and the dashed arrow for the spin ordering. Panel (d) shows the peak positions as a function of temperature.

larizations. To facilitate a comparison of the lineshape, panels (c) and (d) show the same data as given in (a) and (b), but this time normalized to the area. As can be observed in Fig. 2, I_π and I_σ are of very similar magnitude and exhibit the same lineshapes for $150 \text{ K} < T < 200$ K, i.e., $I_\pi \simeq I_\sigma$ for the orbital $(1/2, 0, 0)_{D1}$ peak. The situation clearly changes at 150 K upon cooling: while I_π shows a strong increase by a factor of ~ 10 accompanied by a clear lineshape change, I_σ remains almost unaltered. Furthermore, whereas the peak in I_π apparently shifts in position, as described above (cf. Fig. 1), the peak in I_σ does not move at T_N . From this we conclude that the additional magnetic scattering below T_N , which corresponds to $(0, 1/2, 0)_{D2}$ of $D2$, is almost entirely restricted to I_π , whereas I_σ is due to the orbital $(1/2, 0, 0)_{D1}$ peak of $D1$.

Surprisingly, we observe another dramatic change of the RSXS linshapes at $T_2 = 75$ K well below T_N . This time, I_σ displays clear changes of lineshape and intensity, as shown in Figs. 2 (b) and (d). The variation of I_σ across T_2 signals a third phase transition, which has not been reported earlier and is absent in the bulk material.

The phase transitions at T_N and T_2 are also clearly revealed by the data presented in Fig. 3 (a), which shows I_π and I_σ integrated over the Mn $2p_{3/2}$ and $2p_{1/2}$ regions. In these three panels, one can see a large increase of the total scattering intensity by a factor of more than 10 in I_π around 150 K. This demonstrates the sensitivity of the RSXS-intensity in going from orbital to orbital plus spin order. I_σ increases strongly around $T_2 = 75$ K.

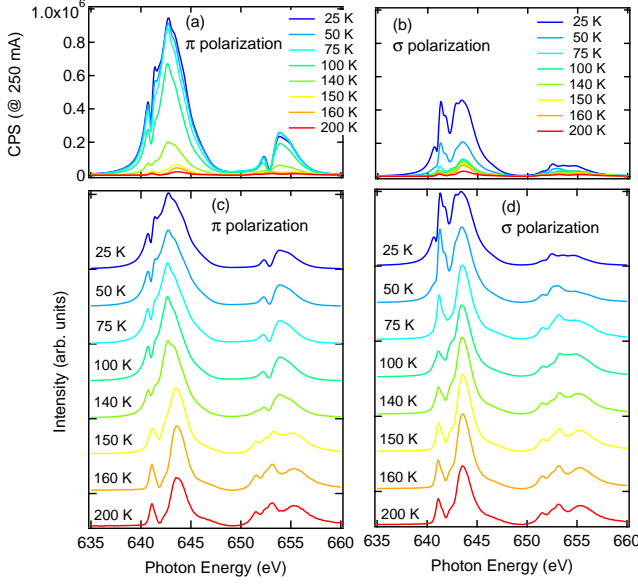


FIG. 2: (Color online) Photon-energy dependence of the $(1/2, 0, 0)/(0, 1/2, 0)$ peak intensity at Mn $2p$ edges at various temperatures using π polarization (a) and σ polarization (b). To compare lineshapes, all data in the panel (a) and (b) have been normalized to each spectrum area, shown at the respective panel (c) and (d) as a function of photon energies.

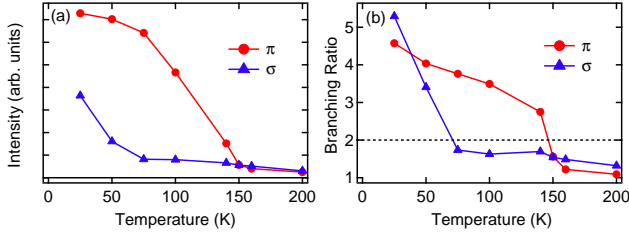


FIG. 3: (Color online) The integrated intensities of the $(1/2, 0, 0)/(0, 1/2, 0)$ peak over both the Mn $2p_{3/2}$ and Mn $2p_{1/2}$ regions (a) and the branching ratio (b), where a statistical value of 2 is also indicated by the dash line.

The changes of the lineshapes at T_N and T_2 become even more apparent by plotting the so-called branching ratio in Fig. 3 (b). Branching ratios are defined by the intensity contributions from the Mn $2p_{3/2}$ region divided by that from the Mn $2p_{1/2}$ region. Since the Mn $2p_{3/2}$ and $2p_{1/2}$ states have 4 and 2 states, respectively, the statistical values of branching ratios are 2, but this value changes due to the local crystal fields, orbital ordering as well as the spin orientation in the ordered system [15]. The branching ratios change strongly around 150 K for a π polarization, and similarly around 75 K for a σ polarization.

In order to gain a better understanding of the experimental results, we have investigated the resonant struc-

ture factor F at the Mn $2p$ edges. Referring to the standard model of the CE-phase, we describe the so-called Mn $^{3+}$ -sites within a local D_{4h} -symmetry, which corresponds to the occupied orbital, while the local symmetry of the so-called Mn $^{4+}$ -sites is taken to be O_h (cf. Fig. 1). Note, that the present model refers to local symmetries only and does not make any assumptions regarding the charge disproportionation in the CE-phase.

The resonant scattering length of a given site n can be expressed as $f_n = \mathbf{e}_f^\dagger \cdot \hat{f}_n(\hbar\omega, \hat{\mathbf{s}}) \cdot \mathbf{e}_i$, with $\hbar\omega$ the photon energy, $\hat{\mathbf{s}} = (s_x, s_y, s_z)$ the direction of the local spin, and \mathbf{e}_i (\mathbf{e}_f) the polarization of the incident (scattered) beam. For the \hat{f}_n in O_h and D_{4h} we use formulae given in Ref. [16], which express the (3×3) -matrixes \hat{f}_n in terms of a few fundamental spectra $f_{n,j}^{(k)}(\hbar\omega)$ with $k = 0, 1, 2, 3$. At the Mn $2p_{3/2,1/2}$ resonance, the scattering is completely dominated by the Mn-sublattice. We therefore calculate the resonant structure factor matrix $\hat{F}(\mathbf{Q}) = \sum_n \hat{f}_n \exp(i\mathbf{Q} \cdot \mathbf{r}_n) = \sum_{k=0}^3 \hat{F}^{(k)}(\mathbf{Q})$ by summing over the 16 Mn-sites of the CE-supercell. Here, $\hat{F}^{(k)}$ only contains fundamental spectra with fixed k . The scattering amplitude and intensity for given \mathbf{e}_i and \mathbf{e}_f can then be calculated as $A_{if} = \mathbf{e}_i^\dagger \cdot \hat{F} \cdot \mathbf{e}_f$ and $I_{if} \propto |A_{if}|^2$, respectively.

For $T_{\text{CO/OO}} > T > T_N$, i.e., for orbital order without spin order, the calculated scattering amplitudes of the orbital $(1/2, 0, 0)$ reflection are $A_{\sigma\sigma'}^{orb} = A_{\pi\pi'}^{orb} = 0$ and $A_{\sigma\pi'}^{orb} = A_{\pi\sigma'}^{orb} \propto (f_{a1g,x}^{(0)} - f_{a1g,y}^{(0)})$, where $f_{a1g,x}^{(0)}$ and $f_{a1g,y}^{(0)}$ are fundamental spectra with $k = 0$. These spectra describe the anisotropy with respect to the local C_4 -axis in D_{4h} , i.e., the anisotropy for polarizations along or perpendicular to the occupied orbital at the Mn $^{3+}$ -sites. The calculation gives $\sigma\pi'$ - and $\pi\sigma'$ -scattering only and yields $I_\pi = I_\sigma$, which is identical to previous results and in good agreement with the present experiment.

A more interesting situation arises when orbital and magnetic order coexist ($T < T_N$). In this case, the structure factor of the orbital order reflection is of the form $\hat{F}_{orb} = \hat{F}_{orb}^{(0)} + \hat{F}_{orb}^{(2)}(\hat{\mathbf{s}})$ ($\hat{\mathbf{s}}$: easy axis). Somewhat surprising, the above equation shows that the spin order can change the resonant scattering at the orbital ordering peak, even though it does not correspond to the magnetic ordering wave vector. These additional contributions are related to the magnetic linear dichroism in XAS and are even in $\hat{\mathbf{s}}$ [16]. On first sight, the spin-dependent $F_{orb}^{(2)}$ might explain the observed dramatic changes of I_π below T_N . However, as discussed above, the shift in position accompanying the increase of I_π implies that the additional intensity has to be attributed to the magnetic $(0, 1/2, 0)$ superlattice peak. The structure factor of this magnetic reflection is given by $\hat{F}_{mag} = \hat{F}_{mag}^{(1)}(\hat{\mathbf{s}}) + \hat{F}_{mag}^{(3)}(\hat{\mathbf{s}})$. These terms are related to the circular magnetic dichroism in XAS [16], i.e., the $(0, 1/2, 0)$ reflection is given by terms odd in $\hat{\mathbf{s}}$ as it should be.

Comparing F_{orb} and F_{mag} to the experimental data a

number of important conclusions can be drawn: Since the orbital scattering in I_σ due to the $(1/2, 0, 0)_{D1}$ peak does not change much for $T_2 < T < T_{CO/OO}$, it is still dominated by same fundamental spectra $f_{a1g,x}^{(0)}$ and $f_{a1g,y}^{(0)}$ at these temperatures. In contrast to this, the lineshape in I_π does change dramatically with the onset of magnetic order, due to the strong additional magnetic intensity stemming from the $(0, 1/2, 0)_{D2}$ peak. The changed lineshape is easily explained qualitatively by the different fundamental spectra, which enter \hat{F}_{orb} and \hat{F}_{mag} .

Furthermore, the experimental results show that for $T_N > T > T_2$ the magnetic intensity is almost exclusively confined to I_π , while there is almost no magnetic scattering in I_σ . This very specific feature of the magnetic scattering provides information about the spin directions in this temperature range: We first note that, since $|f_{n,j}^{(k=3)}| \ll |f_{n,j}^{(k=1)}|$ (cf. Ref. [16]), we can take the approximation $\hat{F} = \hat{F}^{(1)}$, which yields

$$\begin{aligned} \sqrt{3} A_{\sigma\pi'}^{mag} = & f_{a2u}^{(1)} \left((2 + 3\sqrt{2}) s_x + (3\sqrt{2} - 2) s_y \right) \\ & + f_{eu}^{(1)} \left((2 + 3\sqrt{2}) s_x + (3\sqrt{2} - 2) s_y + 4s_z \right) \end{aligned}$$

$s_{x,y,z}$ refer to the x, y, z -axes indicated in Fig. 1. No magnetic scattering in I_σ means that $A_{\sigma\pi'}^{mag} = 0$ at all photon energies. Since $f_{a2u}^{(1)}$ and $f_{eu}^{(1)}$ are linear independent, their coefficients must vanish in this case, which implies that $s_z = 0$ and $s_y/s_x = (2 + 3\sqrt{2})/(2 - 3\sqrt{2})$ and corresponds to an easy axis close to $\hat{s}_0 = (\cos \phi, \sin \phi, 0)$ with $\phi = 110^\circ$. Note that the spin orientation determines how the different fundamental spectra contribute to the total intensity. We therefore conclude that the dramatic changes of I_σ below T_2 are due to a spin reorientation, which results in $A_{\sigma\pi'} \neq 0$. This additional spin reorientation clearly indices that the epitaxial strain changes the magnetic anisotropy of PCMO.

Finally we note that for spins close to \hat{s}_0 the term $F_{orb}^{(2)}$ should result in additional contributions to I_σ as well. But since the lineshape of I_σ remains largely unaltered across T_N , the data indicates that these contributions are significantly smaller than the ones given by $F_{orb}^{(0)}$.

In summary, we performed RSXS studies of the orbital and magnetic order in $\text{Pr}_{0.5}\text{Ca}_{0.5}\text{MnO}_3$ thin films grown on LSAT (011)_c substrates. The different scattering angles together with the polarization and energy dependent lineshapes enable us to separate the orbital and magnetic scattering originating from different twin domains. In addition to the orbital order and spin order transitions known from bulk materials, we observe a third spin reorientation transition at T_2 that is absent in bulk materials. Importantly, the magnetic $(0, 1/2, 0)$ -modulation of the PCMO-film is different from the $(0, 1/2, 1)$ -modulation of the conventional bulk CE-phase: in contrast to bulk materials, the film exhibits ferromagnetic correlations along the c -axis. We also deduce a different magnetic easy

axis for the film as compared to the bulk. These differences between the PCMO-film and the corresponding bulk material indicate a direct coupling of the epitaxial strain to the magnetism. This coupling is most likely mediated by the orbital degree of freedom, which couples strongly to both the lattice and the spin system, thereby providing a convenient route to tune the magnetic properties of manganite films by epitaxial strain. Furthermore, the presented analysis demonstrates that detailed information can be obtained from RSXS measurements already from arguments that are solely based on local symmetries. Even more information, however, could be extracted from a detailed lineshape analysis. The present study is the first demonstration of the antiferromagnetic ordering below 150 K in $\text{Pr}_{0.5}\text{Ca}_{0.5}\text{MnO}_3$ thin films. Since the volume of thin films is very small, it is difficult to study magnetism of thin films by neutron diffraction. Our results demonstrate that RSXS is a very suitable experimental technique to study magnetic order of thin film materials.

H. Wadati and J. Geck contributed equally to this work. The authors would like to thank Y. Wakabayashi, U. Staub, A. Tanaka, and J. Okamoto for informative discussions. This research was made possible with financial support from the Canadian funding organizations NSERC, CFI, and CIFAR and is granted by the Japan Society for the Promotion of Science (JSPS) through the ‘‘Funding Program for World-Leading Innovative R&D on Science and Technology (FIRST Program)’’, initiated by the Council for Science and Technology Policy (CSTP). J. Geck gratefully acknowledges the support through the DFG Emmy Noether Program (Grant GE-1647/2-1).

* Electronic address: wadati@ap.t.u-tokyo.ac.jp;
URL: <http://www.geocities.jp/qxbqd097/index2.htm>

- [1] M. Imada, A. Fujimori, and Y. Tokura, Rev. Mod. Phys. **70**, 1039 (1998).
- [2] A. P. Ramirez, J. Phys.: Condens. Mat. **9**, 8171 (1997).
- [3] Y. Tokura and N. Nagaosa, Science **288**, 462 (2000).
- [4] C. N. R. Rao, A. Arulraj, A. K. Cheetham, and B. Raveau, J. Phys.: Condens. Mat. **12**, R83 (2000).
- [5] W. Prellier, P. Lecoeur, and B. Mercey, J. Phys.: Condens. Mat. **13**, R915 (2001).
- [6] E. Dagotto, T. Hotta, and A. Moreo, Phys. Rep. **344**, 1 (2001).
- [7] A. M. Haghiri-Gosnet and J. P. Renard, J. Phys. D: Appl. Phys. **36**, R127 (2003).
- [8] Y. Tokura, Rep. Prog. Phys. **69**, 797 (2006).
- [9] Z. Jirak, S. Krupicka, Z. Simsa, M. Dlouha, and S. Vratilav, J. Magn. Magn. Mater. **53**, 153 (1985).
- [10] A. Daoud-Aladine, J. Rodriguez-Carvajal, L. Pinsard-Gaudart, M. T. Fernandez-Diaz, and A. Revcolevschi, Phys. Rev. Lett. **89**, 097205 (2002).
- [11] D. V. Efremov, J. van den Brink, and D. I. Khomskii, Nature Mater. **3**, 853 (2004).

- [12] M. Nakamura, Y. Ogimoto, H. Tamaru, M. Izumi, and K. Miyano, Appl. Phys. Lett. **86**, 182504 (2005).
- [13] D. Okuyama, M. Nakamura, Y. Wakabayashi, H. Itoh, R. Kumai, H. Yamada, Y. Taguchi, T. Arima, M. Kawasaki, and Y. Tokura, Appl. Phys. Lett. **95**, 152502 (2009).
- [14] D. G. Hawthorn, F. He, L. Venema, H. Davis, A. J. Achkar, J. Zhang, R. Sutarto, H. Wadati, A. Radi, T. Wilson, G. Wright, K. M. Shen, J. Geck, H. Zhang, V. Novak, and G. A. Sawatzky, Rev. Sci. Instr. **82**, 073104 (2011).
- [15] B. T. Thole and G. van der Laan, Phys. Rev. B **38**, 3158 (1988).
- [16] M. W. Haverkort, N. Hollmann, I. P. Krug, and A. Tanaka, Phys. Rev. B **82**, 094403 (2010).